

# An emission mechanism explaining off-pulse emission originating in the outer magnetosphere of pulsars.

Rahul Basu<sup>1</sup>, Dipanjan Mitra<sup>1</sup> and George I Melikidze<sup>2</sup>

<sup>1</sup>*National Centre for Radio Astrophysics, P. O. Bag 3, Pune University Campus, Pune: 411 007. India*

<sup>2</sup>*Kepler Institute of Astronomy, University of Zielona Góra, Lubuska 2, 65-265, Zielona Góra, Poland*

rbasu@ncra.tifr.res.in, dmitra@ncra.tifr.res.in, gogi@astro.ia.uz.zgora.pl

## ABSTRACT

We have examined the cyclotron resonance instability developing in the relativistic outflowing plasma in the pulsar magnetosphere. The instability condition leads to radio emission in the sub-GHz frequency regime which is likely to be seen as off-pulse emission. Recent studies have shown the presence of off-pulse emission in long period pulsars, and we demonstrate this plasma process to be an energetically viable mechanism.

*Subject headings:* pulsars: general — radiation mechanisms: general — plasmas — pulsars: individual (B0525+21, B2045-16)

## 1. Introduction

The cyclotron resonance instability in relativistic plasma which leads to cyclotron maser emission has been proposed as a feasible mechanism for generating coherent emission at low radio frequencies in many astrophysical systems. The emission mechanism works in plasma systems where excess free energy in the particle distribution is unable to dissipate internally. The excess energy is directly emitted as electromagnetic radiation through a mechanism of negative absorption in the plasma, equivalent to a maser-like emission. The cyclotron resonance instability is expected to be the source of radio emission in a large number of space plasmas and astrophysical systems like the auroral kilometric radiation of the Earth, the auroral emission in Jupiter, Saturn and exoplanets, spikes in radio emission from Sun and stars at low radio frequencies, coherent radiation from blazar jets, and so on (Treumann 2006).

The cyclotron resonance instability has been suggested as a possible mechanism for the coherent main pulse emission in pulsars (Kazbegi et al. 1987, 1991). Electromagnetic waves in the radio frequency regime, excited as a result of this emission mechanism, originate in the outer mag-

netosphere nearer to the light cylinder. However observations in the recent past have constrained the main pulse emission to originate near the neutron star surface at a height of  $\sim 500$  km, about 1% the light cylinder distance (Rankin 1993a,b; Kijak & Gil 1998, 2003; Mitra & Rankin 2002). This rules out the cyclotron resonance instability as a suitable emission mechanism for the main pulse.

Recent discoveries have shown the presence of coherent radio emission in the pulsar profile far away from the main pulse (Basu et al. 2011, 2012). The coherent emission from pulsars is generated in the relativistic plasma flowing outward from the stellar surface along the open magnetic field lines. The main pulse is observationally constrained to originate near the pulsar surface, thereby compelling any off-pulse emission far away from it to originate in the outer magnetosphere. In this paper we assess the plasma conditions necessary for the cyclotron resonance instability to develop in the outer magnetosphere and whether it can account for the detected off-pulse emission. In §2 we describe the general conditions in the pulsar magnetosphere leading to radio emission. §3 describes the condition for the cyclotron resonance instability to develop in the pulsar magnetosphere and its

applicability to off-pulse emission. §4 deals with the energetics of the emission mechanism followed by a short discussion in §5 about the implications of this mechanism to pulsar radio emission.

## 2. Radio emission in Pulsars

In this section we briefly describe the conditions in the pulsar magnetosphere leading to radio emission. Most of the models explaining the emission mechanism involve the presence of an inner acceleration region above the polar cap leading to the formation of dense outflowing  $e^-e^+$  plasma. We explore below the mechanism first described by Ruderman & Sutherland (1975); hereafter RS75; and later modified by Gil & Sendyk (2000) called the “sparking” vacuum-gap model.

The neutron star, radius  $R_S = 10^6$  cm, is characterized by a strong magnetic field  $B_s$ , which is highly multipolar near the stellar surface. The dipole part of the surface magnetic field is given as  $B_d = 3.2 \times 10^{19} (P\dot{P})^{1/2}$  G, here  $P$  and  $\dot{P}$  are the rotation period and period derivative, respectively,  $B_s = bB_d$  and  $b \gg 1$ . The rotating magnetic field gives rise to an electric field ( $\mathbf{E}$ ), and in order to maintain the force-free condition ( $\mathbf{E} \cdot \mathbf{B} = 0$ ) a corotating charge-separated magnetosphere, with density  $n_{GJ} = -(\mathbf{\Omega} \cdot \mathbf{B})/2\pi c\mathbf{e}$  (Goldreich & Julian 1969), surrounds the neutron star. The force-free condition breaks down at the light cylinder,  $R_{LC} = c/\Omega \approx 4.8 \times 10^9 P$  cm, beyond which the charges no longer corotate. Above the polar regions there is an outflow of charges and the magnetosphere slowly recedes, resulting in a charge depleted vacuum gap with a large potential drop across it. In the gap region  $e^-e^+$  pairs are created by pair production involving background  $\gamma$ -ray photons interacting with the high magnetic field. The pairs so created are accelerated in opposite directions to relativistic energies by the large potential difference across the gap. These highly energetic particles produced in the vacuum gap emit further  $\gamma$ -rays via curvature radiation and/or inverse Compton scattering, giving rise to a cascade of  $e^-e^+$  pairs which discharges the potential difference across the gap. The height of the gap region  $h$  stabilizes at the mean free path length of the  $\gamma$ -ray photons and is given by RS75 as:

$$h = 5 \times 10^3 b^{-4/7} P^{1/7} \dot{P}_{-15}^{-2/7} \rho_6^{2/7} \text{ cm.}$$

Here  $\rho_6 = \rho/10^6$  cm, where  $\rho$  is the radius of curva-

ture of the multipolar field lines in the gap region. The potential difference across the vacuum gap is  $\Delta V = \Omega B h^2/c$  which, according to RS75, reduces to:

$$\Delta V = 5 \times 10^9 b^{-1/7} P^{-3/14} \dot{P}_{-15}^{-1/14} \rho_6^{4/7} \text{ Volts.}$$

The discharge of the vacuum gap takes place through a series of sparks which deposit highly energetic singly charged primary particles beyond the gap region. According to the “sparking” model (Gil & Sendyk 2000) the typical diameters of the sparks are  $\sim h$ . The primary particles have maximum energies specified as  $\gamma_b = e\Delta V/mc^2 \sim 3 \times 10^6$  for typical pulsar parameters. Due to partial shielding of the acceleration region by thermionic ions, the gap potential drops to  $\Delta V = \eta \Delta V_{max}$  (Gil et al. 2003), and the particle densities are given as  $n_b = \eta n_{GJ}$ , where  $0 < \eta < 1$  is the screening factor. Once outside the gap the primary particles cease to accelerate but continue emitting curvature radiation with characteristic photon energies given by  $\hbar\omega_c = \frac{3}{2}\gamma_b^3 \hbar c/\rho$ . The photons continue pair production resulting in a cloud of secondary  $e^-e^+$  plasma with typical energies  $\gamma_p = \hbar\omega_c/2mc^2 \sim 10$ -1000 and density  $n_p = \chi n_{GJ}$ , where  $\chi \sim 10^4$  is the Sturrock multiplicative factor (Sturrock 1971). The spark discharge timescale in the vacuum gap is a few tens of  $\mu$ seconds, and this results in overlapping clouds of outflowing secondary plasma penetrated by the primary particles. Thus to summarize, the pulsar magnetosphere above the polar cap consists of a series of secondary plasma clouds, each corresponding to a “spark” in the vacuum gap, penetrated by primary particles, moving outward along the magnetic field.

The principal predicament in explaining the radio emission from pulsars is its coherent nature evidenced by high brightness temperatures. This presages the presence of a bunching mechanism resulting in a large number of charged particles radiating simultaneously in phase. There are two possible regions where instabilities in the outflowing plasma can lead to charge bunching. In the first case particles of different momenta in the overlapping clouds undergo two stream instability giving rise to strong electrostatic Langmuir waves around heights of  $\sim 50R_S$ . The Langmuir waves are modulationally unstable, and nonlinear plasma processes results in bunching of charged solitons (Melikidze et al. 2000). The ra-

dio emission from the main pulse originates around these heights (Rankin 1993a,b; Kijak & Gil 1998, 2003; Mitra & Rankin 2002) and is explained as curvature radiation from the charged solitons (Gil, Lyubarsky & Melikidze 2004). In the second case the naturally developing electromagnetic modes in the clouds of secondary plasma undergo negative absorption from the highly energetic primary particles via the cyclotron resonance instability (Kazbegi et al. 1987, 1991; Lyutikov et al. 1999) with the possibility of coherent radio emission. Such an emission near the light cylinder will likely be spread out over a large part of the pulsar's rotation cycle and is a likely source of off-pulse emission. In the next sections we examine the conditions necessary for the development of the cyclotron resonance instability near the light cylinder and its viability in explaining the detected off-pulse emission.

### 3. Conditions for emission near the light cylinder

The magnetic field near the outer magnetosphere becomes strictly dipolar field due to the much faster decay of the higher multipoles. The magnetic field and plasma density, within the dipolar structure, decrease with distance from neutron-star surface as  $(R_S/R)^3$ . The high magnetic field near the neutron-star surface constrains the outflowing plasma to move along the field lines. This condition is relaxed near the light cylinder where the magnetic field is much weaker and the particles are able to gyrate. Within the outflowing plasma various electromagnetic (EM) propagating modes can be generated. The extra-ordinary mode is one such example which is a transverse EM wave capable of propagating in the plasma and escaping the plasma region. The dispersion relation for the extra-ordinary waves is given as (Kazbegi et al. 1991):

$$\omega = kc(1 - \delta), \quad \delta = \frac{\omega_p^2}{4\omega_B^2\gamma_p^3} \quad (1)$$

Here  $\omega_B$  is the cyclotron frequency and  $\omega_p$  the plasma frequency.

$$\omega_B = \frac{eB}{m_e c}; \quad \omega_p = \left( \frac{4\pi n_p e^2}{m_e} \right)^{1/2} \quad (2)$$

The amplitude of the extra-ordinary wave should grow as it propagates through the plasma if it is

to escape the plasma region. This amplification is provided by the high energy primary plasma through the cyclotron resonance instability. The primary particles near the light cylinder are capable of resonating with the extra-ordinary wave. The particles in addition also undergo curvature drift with a drift velocity  $u_d = \gamma c^2 / \omega_B \rho$ . The resonance condition for the instability is given as:

$$\omega(\mathbf{k}) - k_{\parallel} v_{\parallel} - k_{\perp} u_d + \frac{\omega_B}{\gamma} = 0. \quad (3)$$

The dispersion relation [eq.(1)] and the resonance condition [eq.(3)] gives the resonance frequency to be

$$\omega_0 = \frac{\omega_B}{\gamma_{res} \delta}. \quad (4)$$

Here  $\gamma_{res} = \gamma_b$ . In addition to the excitation of resonance frequency, another factor that is crucial for the emergence of the emission is the growth rate  $\Gamma$  specified as (Kazbegi et al. 1991):

$$\begin{aligned} \Gamma &= \pi \frac{\omega_{p,res}^2}{\omega_0 \gamma_T} & u_d^2 / 2c^2 \delta &\ll 1 \\ \Gamma &= \pi \frac{\omega_{p,res}^2}{2\omega_0 \gamma_T} \frac{u_d^2}{c^2 \delta} & u_d^2 / 2c^2 \delta &\gg 1 \end{aligned} \quad (5)$$

$\gamma_T$  is the thermal spread in the primary particle distribution. The necessary conditions for the electromagnetic emission due to the cyclotron resonance instability are:

1. The growth factor should be large  $\Gamma\tau > 1$ , where  $\tau \sim R_{LC}/c = P/2\pi$  is the growth time, i.e. the duration before the waves escape the light cylinder.
2. The resonance frequency should not exceed the damping frequency,  $\omega_0 < \omega_1 = 2\gamma_p \omega_B$ .

#### 3.1. Parametric representation

We assume the emission to manifest at the light cylinder,  $R_{LC} = c/\Omega \approx 4.8 \times 10^9 P$  cm, ensuring maximum growth of the resonant waves. We determine a representation of the conditions explained above in terms of the basic parameters of the pulsar and the outflowing plasma. The magnetic field is given as:

$$\begin{aligned} B &\approx 10^{12} (P \dot{P}_{-15})^{1/2} (R_S/R)^3 \text{ G} \\ &\approx 9 (\dot{P}_{-15}/P^5)^{1/2} \text{ G} \end{aligned} \quad (6)$$

Here  $R_S \sim 10^6$  cm and  $B$  is represented at the light cylinder. The Goldreich-Julian density on the neutron star surface is given as

$$\begin{aligned} n_{GJ} &= -(\mathbf{\Omega} \cdot \mathbf{B})/2\pi ce \\ &\approx 6.9 \times 10^{10} (\dot{P}_{-15}/P)^{1/2} \text{ cm}^{-3} \end{aligned} \quad (7)$$

Using eq.(6) and (7) and appropriate distance scaling, the various plasma properties at the light cylinder are as follows.

$$\begin{aligned} \omega_p^2 &\approx 4.1 \times 10^9 \chi \left( \frac{\dot{P}_{-15}}{P^7} \right)^{1/2} \\ \omega_{p,res}^2 &\approx 4.1 \times 10^9 \eta \left( \frac{\dot{P}_{-15}}{P^7} \right)^{1/2} \\ \omega_B &\approx 3.3 \times 10^8 \left( \frac{\dot{P}_{-15}}{P^5} \right)^{1/2} \\ \delta &\approx 9.6 \times 10^{-9} \left( \frac{\chi}{\gamma_p^3} \right) \left( \frac{P^3}{\dot{P}_{-15}} \right)^{1/2} \end{aligned} \quad (8)$$

The frequency of the emitted waves and the damping frequency follows from eq.(8).

$$\begin{aligned} \omega_0 &\approx 3.4 \times 10^{16} \left( \frac{\gamma_p^3}{\chi \gamma_{res}} \right) \left( \frac{\dot{P}_{-15}}{P^4} \right) \\ \omega_1 &\approx 6.5 \times 10^8 \gamma_p \left( \frac{\dot{P}_{-15}}{P^5} \right)^{1/2} \end{aligned} \quad (9)$$

In order to determine the growth condition we need to look into the relevance of the curvature drift. At the light cylinder  $\rho \sim R_{LC}$ , hence the drift velocity and drift condition are given as

$$\begin{aligned} u_d &\approx 5.7 \times 10^2 \gamma_{res} \left( \frac{P^3}{\dot{P}_{-15}} \right)^{1/2} \\ \frac{u_d^2}{2c^2\delta} &\approx 1.9 \times 10^{-8} \left( \frac{\gamma_{res}^2 \gamma_p^3}{\chi} \right) \left( \frac{P^3}{\dot{P}_{-15}} \right)^{1/2} \end{aligned} \quad (10)$$

For typical pulsar parameters it can be shown that  $u_d^2/c^2\delta \gg 1$ , establishing the importance of curvature drift. The growth factor using the second part of eq.(5) is

$$\Gamma\tau \approx 1.2 \times 10^{-15} \left( \frac{\eta \gamma_{res}^3}{\gamma_T} \right) \left( \frac{P^3}{\dot{P}_{-15}} \right) \quad (11)$$

Finally the limits on frequency,  $\omega_0 < \omega_1$ , and growth factor,  $\Gamma\tau > 1$ , constrains the pulsar and plasma parameters.

$$\begin{aligned} \left( \frac{\chi \gamma_{res}}{\gamma_p^2} \right) \left( \frac{P^3}{\dot{P}_{-15}} \right)^{1/2} &> 5.2 \times 10^7 \\ \left( \frac{\eta \gamma_{res}^3}{\gamma_T} \right) \left( \frac{P^3}{\dot{P}_{-15}} \right) &> 8.3 \times 10^{14} \end{aligned} \quad (12)$$

The conditions for the emission are shown in Fig. 1 for the pulsar population in the  $P\dot{P}$  diagram.

### 3.2. Application to off-pulse emission

We now look into the application of the parametric formulation for a specific set of pulsar parameters and apply them to two pulsars with detected off-pulse emission. The pulsar parameters used for our studies are,  $\gamma_p = 10$ ;  $\chi = 10^4$ ;  $\gamma_{res} = 2 \times 10^6$ ;  $\gamma_T = 10^2$ ;  $\eta = 10^{-1}$ . We look at the various conditions as explained above.

$$\frac{u_d^2}{2c^2\delta} \approx 7.6 \times 10^2 \left( \frac{P^3}{\dot{P}_{-15}} \right)^{1/2} \quad (13)$$

$$\nu_0 = \omega_0/2\pi \approx 270 \left( \frac{\dot{P}_{-15}}{P^4} \right) \text{ MHz} \quad (14)$$

$$\nu_1 = \omega_1/2\pi \approx 1.03 \left( \frac{\dot{P}_{-15}}{P^5} \right)^{1/2} \text{ GHz} \quad (15)$$

$$\Gamma\tau \approx 9.3 \left( \frac{P^3}{\dot{P}_{-15}} \right) \quad (16)$$

**B0525+21:**  $P = 3.7455$  sec;  $\dot{P}_{-15} = 40.05$ ;  
The limits expressed in eq.(12) reduce to

$$\begin{aligned} \left( \frac{\chi \gamma_{res}}{\gamma_p^2} \right) \left( \frac{P^3}{\dot{P}_{-15}} \right)^{1/2} &= 2.3 \times 10^8 > 5.2 \times 10^7 \\ \left( \frac{\eta \gamma_{res}^3}{\gamma_T} \right) \left( \frac{P^3}{\dot{P}_{-15}} \right) &= 1.05 \times 10^{16} > 8.3 \times 10^{14} \end{aligned}$$

**B2045-16:**  $P = 1.9616$  sec;  $\dot{P}_{-15} = 10.96$ ;  
The limits expressed in eq.(12) reduce to

$$\begin{aligned} \left( \frac{\chi \gamma_{res}}{\gamma_p^2} \right) \left( \frac{P^3}{\dot{P}_{-15}} \right)^{1/2} &= 1.7 \times 10^8 > 5.2 \times 10^7 \\ \left( \frac{\eta \gamma_{res}^3}{\gamma_T} \right) \left( \frac{P^3}{\dot{P}_{-15}} \right) &= 5.5 \times 10^{15} > 8.3 \times 10^{14} \end{aligned}$$

The pulsar parameters for the two pulsars have been obtained from the ATNF pulsar database (Manchester et al. 2005).

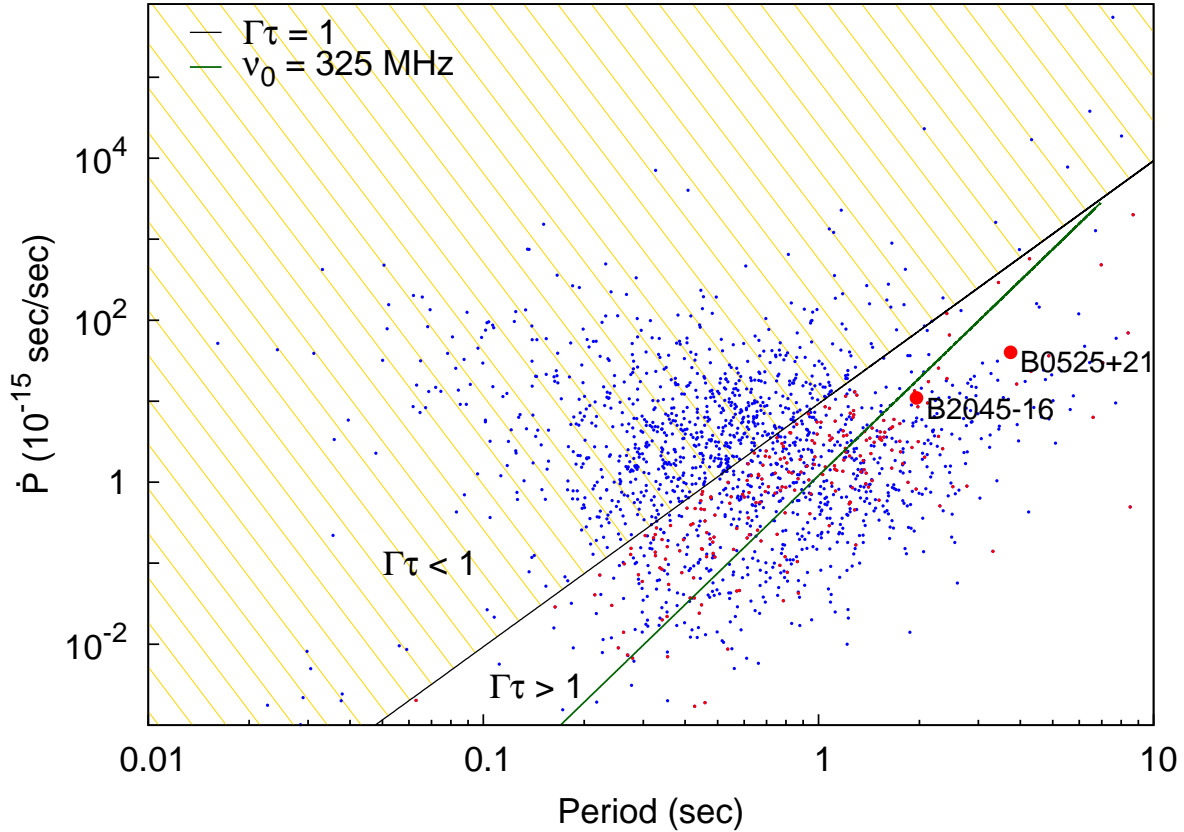


Fig. 1.— The condition for cyclotron resonance instability for the pulsar population (red and blue points) is represented in the  $P\dot{P}$  diagram with the relevant pulsar parameters given in §3.2. The solid black line corresponds to eq.(16) where the growth factor  $\Gamma\tau = 1$ . The instability condition develops in the pulsar population where  $\Gamma\tau > 1$  [eq.(16)]. The region where  $\Gamma\tau < 1$  (shaded region) represents the pulsars (blue points in shaded region) where radio emission in outer magnetosphere cannot originate. For the pulsar parameters assumed for our calculations (§3.1 and 3.2) the resonance frequency of emission at 325 MHz [eq.(14)] is shown as the green line. In addition to satisfying the instability condition (region where  $\Gamma\tau > 1$ ) the possibility of detecting radio emission depends on the flux density and the efficiency of energy in the plasma being converted into radio emission. Using an upper detection limit of 1 mJy for current radio telescopes at the sub GHz range, we estimate the minimum observable luminosity  $L_{obs}$  for each pulsar using eq.(20). Assuming the efficiency of the emission mechanism to be about 5% of  $L_p$  [given by eq.(19)] we find a sub-sample (red points) where the emission mechanism presented here can give rise to detectable off-pulse emission (i.e.  $0.05L_p > L_{obs}$  and  $\Gamma\tau > 1$ ). The two pulsars PSR B0525+21 and PSR B2045-16, where off-pulse emission is observed, lie in the favorable region for cyclotron resonance instability.

As shown in Fig. 1, the two pulsars B0525+21 and B2045–16 which show the presence of off-pulse emission (Basu et al. 2011, 2012) lie in the regime where cyclotron resonance instability is likely to emit observable coherent radio emission. The resonance frequency of emission at 325 MHz given by eq.(14) is shown as a green line in Fig. 1.

In the analysis presented here we have made two basic assumptions that the resonance condition develops at the light cylinder and the secondary plasma is characterized by  $\gamma_p = 10$ . These assumptions, although they demonstrate the viability of the emission mechanism and constrain the parameter space, do not put strict limits on the secondary plasma energy or location of emission in the pulsar magnetosphere. In one scenario for the same pulsar it is possible for the resonance condition to originate at a different height for a slightly different secondary plasma energy, i.e, lower energy particles will emit the same resonance frequency at a lower height. In an alternate picture the same energy particles will satisfy the resonance condition at a different height for a different resonance frequency, i.e, the resonance frequency will be higher at a lower height. In a typical pulsar all these scenarios are likely to exist, which would account for not only the wide range of frequencies likely to be emitted but also the spread of the detected signal over a wide range in the pulsar profile. However the emission conditions can only develop in the outer magnetosphere near the light cylinder, which in conjunction with the damping frequency puts a limit on the maximum frequency that can be emitted to be around the GHz range.

#### 4. Energetics

In this section we look into the total energy available in the plasma and its sufficiency in accounting for the detected off-pulse emission. The total available energy in the plasma when emitted as radio emission gives

$$L_p = \gamma_{res} m c^3 n_{res} \beta_p \quad \text{erg s}^{-1} \quad (17)$$

Here  $\beta_p$  represents the cross-section of the open field lines,  $\beta_p = 6.6 \times 10^8 P^{-1} (R/R_s)^3 \text{ cm}^2$ . The luminosity of the off-pulse emission is given as:

$$L_{obs} = 4\pi D_L^2 S_\nu \Delta\nu \zeta^{-1} \quad \text{erg s}^{-1} \quad (18)$$

Here  $D_L$  is the distance to pulsar;  $S_\nu$  the observed off-pulse flux;  $\Delta\nu$  is the frequency range and  $\zeta$

the fractional opening angle. Using  $\gamma_{res}=2 \times 10^6$ ;  $\eta=10^{-1}$ ;  $S_\nu=1 \text{ mJy}$ ;  $\Delta\nu=100 \text{ MHz}$ ;  $\zeta=10^{-1}$  eq.(17) and (18) are expressed as

$$L_p \approx 2.2 \times 10^{29} \left( \frac{\dot{P}_{-15}}{P^3} \right)^{1/2} \quad (19)$$

$$L_{obs} \approx 1.2 \times 10^{27} D_{kpc}^2 \quad (20)$$

Applying the luminosity values to the two pulsars as in the previous section we look into the relevance of the mechanism.

**B0525+21:**  $D_{kpc} = 2.28$ .  $L_p = 2.5 \times 10^{29}$ ;  $L_{obs} = 6.2 \times 10^{27}$ .

**B2045–16:**  $D_{kpc} = 0.95$ .  $L_p = 1.8 \times 10^{29}$ ;  $L_{obs} = 1.1 \times 10^{27}$ .

$L_p \gg L_{obs}$  for off-pulse emission in both pulsars. It is clear that the cyclotron resonance instability is an energetically viable mechanism for off-pulse emission in the two examples shown.

#### 5. Discussion

In this work we have demonstrated the generation of radio emission due to the cyclotron resonance instability within the outer magnetosphere of pulsars making it a relevant candidate for off-pulse emission. The conditions for radio emission are dependent on the parameters of the plasma which are still poorly understood. The details of the calculations shown here will vary with changes in plasma parameters although the basic physical processes would still operate in pulsars. We can draw two primary conclusions about the nature and extent of the emission from these studies. Firstly, these conditions can only develop in a certain population of pulsars which have longer periods and/or smaller period derivatives. Secondly, there is an upper limit to the frequency that can be emitted constrained by the damping frequency. In addition we have also found an observational limit based on the detection capabilities of present day telescopes and energetics which show the emission from long period pulsars with very small period derivatives generally too weak to be observed. The pulsars which follow the above criteria are shown as red points in Fig. 1 (see figure caption for details).

Further observational results involving a large sample of pulsars in addition to determining the temporal structure, polarization features and the

spectral nature of the off-pulse emission will not only help in validating the mechanism, but will also help in refining its predictions.

We thank the anonymous referee for constructive criticism that helped to improve the paper. We would like to thank Joanna Rankin for carefully reading the manuscript and her helpful comments which improved the manuscript. We also thank Janusz Gil for his useful comments. This work was partially supported through the grant DEC-2012/05/B/ST9/03924 by the Polish National Science Centre.

## REFERENCES

- Basu, R., Athreya, R., Mitra D. 2011, ApJ, 728, 157
- Basu, R., Mitra D., Athreya, R. 2012, ApJ, 758, 91
- Gil, J.A.; Sendyk, M. 2000, ApJ, 541, 351
- Gil, J.; Melikidze, G.I.; Geppert, U. 2003, A&A, 407, 315
- Gil, J.; Lyubarsky, Y.; Melikidze, G.I. 2004, ApJ, 600, 872
- Goldreich, P.; Julian, W.H. 1969, ApJ, 157, 869
- Kazbegi, A.Z.; Machabeli, G.Z.; Melikidze, G.I. 1987, AuJPh, 40, 755
- Kazbegi, A.Z.; Machabeli, G.Z.; Melikidze, G.I. 1991, MNRAS, 253, 377
- Kijak, J.; Gil, J. 1998, MNRAS, 299, 855
- Kijak, J.; Gil, J. 2003, A&A, 397, 969
- Lyutikov, M.; Blandford, R.D.; Machabeli, G. 1999, MNRAS, 305, 338
- Manchester, R.N; Hobbs G.B.; Teoh, A.; Hobbs, M. 2005, AJ, 129, 1993
- Melikidze, G.I.; Gil, J.A.; Pataraya, A.D. 2000, ApJ, 544, 1081
- Mitra, D.; Rankin, J.M. 2002, ApJ, 577, 322
- Mitra, D.; Gil, J.; Melikidze, G.I. 2009, ApJ, 696, 141
- Rankin, J.M. 1993, ApJ, 405, 285
- Rankin, J.M. 1993, ApJS, 85, 145
- Ruderman, M. A., Sutherland, P. G. 1975, ApJ, 196, 51
- Sturrock, P. A. 1971, ApJ, 164, 529
- Treumann, R.A. 2006, A&A Rev., 13, 229